Photoionization of the hydrogen atom: Three-dimensional results and pseudo-one-dimensional model

L. Roso-Franco, A. Sanpera, M. Ll. Pons, and L. Plaja
Departament de Física, Universitat Autònoma de Barcelona, 08193 Bellaterra, Spain
(Received 21 March 1991)

Photoionization of atomic hydrogen by a linearly polarized laser is numerically studied using a method based on an expansion of the wave function in angular-momentum components. The numerical method presented is quite efficient to compute photoionization of three-dimensional atoms. Moreover, the main advantage of the method is that it allows a clear comparison with one-dimensional models. As a consequence, we propose a family of models that have the same complexity as a one-dimensional model, but that are closer to real atoms.

PACS number(s): 32.80.Rm, 32.80.Fb, 42.50.Hz

I. INTRODUCTION

With the availability of very intense laser pulses, giving peak intensities close to or beyond atomic unity, a new experimental domain has recently appeared. Its description implies the study of the interaction of an isolated atom with a laser field so intense that standard perturbation techniques fail. This leads to a set of different, and more exact, approaches to the problem [1]. Obviously, it is generally accepted that a satisfactory description of the laser-atom interaction can be obtained numerically by integrating the Schrödinger equation in the dipole approximation. But, even for a single-electron atom, this is a very difficult problem, and few numerical studies on realistic atoms have been available until now. However, it is been proposed by different authors [2–6] that a first qualitative insight to this problem can be obtained solving one-dimensional models, instead of real three-dimensional atoms.

Until now, one-dimensional models have been understood as first approaches to the problem. It is not yet clear how to distinguish in a one-dimensional model the effects that are intrinsic to the model from the phenomenology that should be expected in a real three-dimensional atom.

We want to present, in this paper, a method to solve real three-dimensional single-electron atoms. The method is based on an expansion of the wave function in spherical harmonics, closely related to other previously published treatments [7,8]. But the central result is that by reducing the number of terms in the expansion we can make a smooth transition from three-dimensional results to one-dimensional models. This helps to clarify which features of the one-dimensional models are meaningful in real atoms and which are intrinsic details of one dimension without projection to real atoms.

II. THEORY

A. Wave equation

We consider the time-dependent Schrödinger equation for the hydrogen atom

$$i\frac{\partial\psi(\mathbf{r},t)}{\partial t}=[H_0(r)+H_I(\mathbf{r},t)]\psi(\mathbf{r},t)\ , \tag{1}$$

where the Hamiltonian of the system has been split into two parts. The H_0 term is the atomic Hamiltonian,

$$H_0(r)=-\tfrac{1}{2}\nabla^2-\frac{1}{r}\ . \tag{2}$$

Observe that, for convenience, atomic units ($m=e=\hbar=1$) have been used throughout. The H_I part of the Hamiltonian accounts for the laser-atom interaction, in the electric dipole approximation,

$$H_I(\mathbf{r},t)=\mathbf{r}\cdot\mathbf{E}(t)\sin\omega_L t\ , \tag{3}$$

where ω_L is the laser frequency and $\mathbf{E}(t)$ is the electric field envelope. In this research we will consider only square envelopes, $\mathbf{E}(t)=\mathbf{E}_0$ during the pulse and zero elsewhere. We also consider a laser linearly polarized along the z axis, $\mathbf{r}\cdot\mathbf{E}(t)=rE(t)\cos\theta$, and we take advantage of the expansion in an angular-momentum basis, as standard in this kind of problems [7,8].

The time-dependent wave function can therefore be expanded as

$$\psi(\mathbf{r},t)=\sum_{l=0}^{\infty}\frac{1}{r}\chi_l(r,t)Y_l^0(\theta)\ . \tag{4}$$

For simplicity only spherical harmonics with $m=0$ have been introduced. This kind of simplified expansion is correct provided that the atom is initially in an $m=0$ state, since a laser polarized linearly along the z axis does not couple states with different m. On the other hand, the decomposition of the radial parts as $r^{-1}\chi_l(r,t)$ is standard in this kind of problems and it is well known that that contributes to simplifying certain forthcoming expressions.

Substituting the expansion (4) into the Schrödinger equation and projecting on particular spherical harmonics, one gets

$$i\frac{\partial}{\partial t}\chi_l(r,t)=\left[-\frac{1}{2}\frac{\partial^2}{\partial r^2}-\frac{1}{r}+\frac{l(l+1)}{2r^2}\right]\chi_l(r,t)+\sum_{l'=0}^{\infty}\langle Y_l^0|rE(t)\cos\theta|Y_{l'}^0\rangle\times\sin(\omega_L t)\chi_{l'}(r,t)\ . \tag{5}$$

We observe that the H_0 part of the Hamiltonian does not couple components with different l. The H_I Hamiltonian, however, couples the lth harmonic with the $(l+1)$th and $(l-1)$th harmonics. The coupling constant is given in terms of the Clebsch-Gordan coefficients

$$\langle Y_l^0|\cos\theta|Y_{l\pm1}\rangle^0=\left[\frac{2l+1}{2(l\pm1)+1}\right]^{1/2}(\langle l,0;1,0|l\pm1,0\rangle)^2\ . \tag{6}$$

Since these coefficients are going to appear many times in the paper, we will introduce a simplified notation, calling them $c_l^{\pm}$, where c_l^+ is the coupling constant between the lth harmonic and the $l+1$ (and analogously for c_l^-):

$$c_l^+=\left[\frac{(l+1)^2}{(2l+3)(2l+1)}\right]^{1/2}, \tag{7a}$$

$$c_l^-=\left[\frac{l^2}{(2l+1)(2l-1)}\right]^{1/2}. \tag{7b}$$

Equation (5) finally becomes

$$i\frac{\partial}{\partial t}\chi_l(r,t)=\left[-\frac{1}{2}\frac{\partial^2}{\partial r^2}-\frac{1}{r}+\frac{l(l+1)}{2r^2}\right]\chi_l(r,t)+rE(t)\sin(\omega_L t)[c_l^+\chi_{l+1}(r,t)+c_l^-\chi_{l-1}(r,t)] \tag{8a}$$

for $l>0$, and for $l=0$

$$i\frac{\partial}{\partial t}\chi_0(r,t)=\left[-\frac{1}{2}\frac{\partial^2}{\partial r^2}-\frac{1}{r}\right]\chi_0(r,t)+rE(t)\sin(\omega_L t)c_0^+\chi_1(r,t)\ . \tag{8b}$$

B. Pseudo-one-dimensional limit

With the expansion in the spherical harmonics basis, we have a precise following of the angular momentum of the system. Of course, in any practical calculation it is necessary to introduce a cutoff in the angular-momentum expansion, considering Eq. (8) from $l=0$ to a maximum value $l_{\max}$. Therefore, depending on the multiphoton order of the process and on the intensity of the radiation, one can also analyze the influence of the dynamics of the cutoff value $l_{\max}$.

Pushing this to the limit we are going to study in the present paper the dynamics of our system when just two angular-momentum components ($l=0$ and 1) are considered. In this case, the differential equations describing the evolution of the system reduce to

$$i\frac{\partial}{\partial t}\chi_s(r,t)=\left[-\frac{1}{2}\frac{\partial^2}{\partial r^2}-\frac{1}{r}\right]\chi_s(r,t)+rE(t)\sin(\omega_L t)c_0^+\chi_p(r,t)\ , \tag{9a}$$

$$i\frac{\partial}{\partial t}\chi_p(r,t)=\left[-\frac{1}{2}\frac{\partial^2}{\partial r^2}-\frac{1}{r}+\frac{1}{r^2}\right]\chi_p(r,t)+rE(t)\sin(\omega_L t)c_1^-\chi_s(r,t)\ , \tag{9b}$$

where the notation χ_s,χ_p has been introduced instead of χ_0 and χ_1.

This model has essentially the same computational complexity as a one-dimensional model, but also has some important differences. Thus we will refer to it as the pseudo-one-dimensional limit of the spherical harmonics expansion. To understand the similarities and differences we will describe in a parallel form the standard one-dimensional models.

C. Standard one-dimensional models

Because three-dimensional numerical simulations, even with linear polarization, imply very long numerical computations, it is generally accepted that a first insight on the ionization phenomenology can be obtained with the use of one-dimensional models.

A lot of very interesting work has been done [2–6,9,10] solving one-dimensional models of the form

$$i\frac{\partial}{\partial t}\psi(x,t)=\left[-\frac{1}{2}\frac{\partial^2}{\partial x^2}+V(x)+xE(t)\sin(\omega_l t)\right]\psi(x,t) \tag{10}$$

for many different choices of the potential $V(x)$, trying to simulate either atoms or ions.

We want to study how our pseudo-one-dimensional model, defined in (9), resembles this standard one-dimensional model (10). The analog of a three-dimensional central potential is a symmetric one-dimensional potential, and the standard one-dimensional analog to angular momentum is parity. Therefore we must introduce well-defined parity wave functions. Defining, as usual,

$$\psi_s(x)=\psi(x)+\psi(-x)\ , \tag{11a}$$

$$\psi_a(x)=\psi(x)-\psi(-x) \tag{11b}$$

for $x>0$, and $\psi_s(0)=2\psi(0)$ and $\psi_a(0)=0$, we easily obtain a symmetric function ψ_s and an antisymmetric one, ψ_a.

Substituting in the one-dimensional Schrödinger equation (10), it is straightforward to find the time evolution equations for ψ_s and ψ_a,

$$i\frac{\partial}{\partial t}\psi_s(x,t)=\left[-\frac{1}{2}\frac{\partial^2}{\partial x^2}+V(x)\right]\psi_s(x,t)+xE(t)\sin(\omega_L t)\psi_a(x,t)\ , \tag{12a}$$

$$\frac{\partial}{\partial t}\psi_a(x,t)=\left[-\frac{1}{2}\frac{\partial^2}{\partial x^2}+V(x)\right]\psi_a(x,t) +xE(t)\sin(\omega_L t)\psi_s(x,t) \quad (12b)$$

where $x>0$.

Now the similitude between (9a) and (9b) and (12a) and (12b) is evident and justifies the name of "pseudo-one-dimensional" given to the limit (9a) and (9b). There is, however, a very important difference between them. In the standard one-dimensional model, the atomic part of the Hamiltonian is the same for both equations. This is not true for the pseudo-one-dimensional model, where the "centrifuge" potential appears in the equation that gives the evolution of the p states. In our opinion this is the crucial point to understand the physical meaning of the one-dimensional models. This also explains why in most of the standard one-dimensional studies the atomic potential $V(x)$ is not simply $1/|x|$ but a more complicated function to avoid the singularity at $x=0$. Perhaps the physical interpretation of these nonsingular potentials is that they are, in some sense, an averaged way to introduce the effect of the "centrifugal" repulsion in the evolution of the antisymmetric part of the wave function.

In conclusion, we consider that the standard one-dimensional models neglect some important part of the physical interaction at the moment they consider the same potential for the symmetric and antisymmetric parts of the wave function. Therefore standard one-dimensional models are only a preliminary approach to have a first insight in the ionization dynamics, and for this qualitative approach it is even better not to try to introduce all the details of the Coulomb potential, but to replace it by a δ potential that leads to a ground state more similar to the hydrogen ground state [11,12].

III. RESULTS

A. Method of solution

We will show in this paper some numerical results on the ionization three-dimensional hydrogen, and will compare them with the results of the pseudo-one-dimensional model. But before commenting on the results we want to explain our numerical method.

With the present expansion of the wave function in the spherical harmonics basis and with the field linearly polarized, instead of having a single partial differential equation in two spatial variables, one has several ordinary differential equations, coupled to each other, but now each one of these equations involves just one spatial variable. Working with a single equation with two spatial variables, say in cylindrical coordinates, one needs to introduce a two-dimensional grid of points that implies huge requirements of numerical storage and long computing times. The advantage of the present method is that we need a one-dimensional grid for each one of the equations involved, and the number of equations is given by the maximum value of the angular momentum, $l_{\max}$. This value is, of course, dependent on the intensity and frequency of the laser field, and also on the initial state of the electron. Therefore a control of the population close to this cutoff is necessary for each computation. In many practical cases this value does not have to be very large. For example, with one- to five-photon ionization starting to form the ground state, and intensities lower than the atomic intensity unit, good results are obtained with 10 or 20 different angular momenta. For wide integration regions— as is the case in ionization studies, where the electron can be far from the nucleus—the difference between 10 or 20, one-dimensional grids and a two-dimensional grid can represent many orders of magnitude. When the electron wave function is spread over many different angular-momentum components, the present expansion does not represent a clear advantage.

For the specific method of solution of the system (8a) and (8b) we have considered a combination of the previously published methods [7,8]. The time evolution of the radial functions has been solved using an implicit Crank-Nicholson scheme. We choose to use a three point formula because it allows us to apply fast algorithms. The coupling with the laser field, i.e., the interaction between different χ_l wave-function components, has been considered in terms of a predictor-corrector method, using between three and six iterations in each interval, with a constant time step. This is, obviously, not the fastest form to compute solutions of this kind of systems, but we clearly prefer an explicit nonunitary algorithm to calculate the influence of the laser field because in this way it is more difficult to introduce spurious solutions due to a too long time interval.

In the calculations, the wave function has been expanded in a basis of 11 spherical harmonics, $l_{\max}=10$. The spatial step is $\delta r=0.1$ a.u., and we have considered radii from δr to $r_{\max}=250$ a.u., for each angular-momentum component, which represents 2500×11 points in the integration grid. The chosen time step was $\delta t=\pi/50$ a.u.; that is a rather short step, but as we said before, this is due to our method of calculating the coupling with the field.

B. Three-dimensional results

We present in this paper numerical results for the ionization of three-dimensional atomic hydrogen by a laser pulse of frequency $\omega_L=0.2$ a.u. (equivalent to a free-space wavelength of 163 nm), with a square envelope, that lasts for ten cycles (314 a.u.). We assume that the laser field is linearly polarized and the atom is initially in its ground state $1s$. This value of the laser frequency corresponds to a three-photon ionization threshold, and has been chosen because there are no intermediate resonances with atomic states.

Computed results for a relatively low-intensity field ($I=E^2=10^{-4}$ a.u.$=3.54\times 10^{12}$ W/cm^{-2}) are shown in Fig. 1 and 2. Figure 1 shows the time evolution of the population of the ground state, the initial state. Figure 2 shows the population of different spherical harmonics components, in particular the populations of the s, p, and d states. Obviously these populations have been integrated over the radial variable,

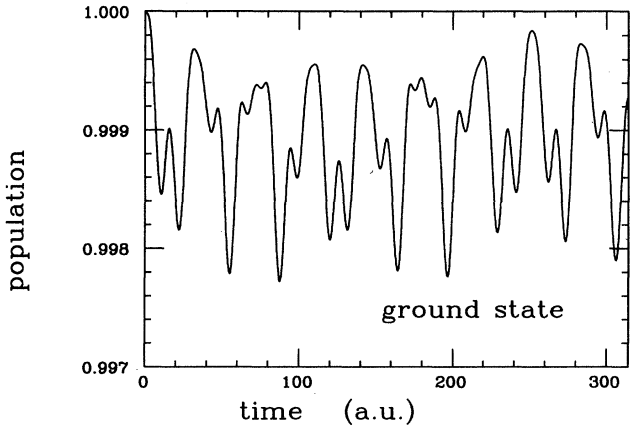

FIG. 1. Time evolution of the ground-state population, for a square laser pulse of frequency $\omega_L=0.2$ a.u. and amplitude $E_0=0.01$ a.u., calculated for a real three-dimensional hydrogen atom and a linearly polarized laser. The pulse lasts only for ten cycles (314 a.u. of time). This pulse is not very intense, therefore only about $\frac{1}{10}\%$ of the population has been removed from the initial state.

$$P_l=\int_0^{r_{\max}}|\chi_l(r,t)|^2dr\ . \tag{13}$$

It is evident that for this low-intensity field almost all the electron population remains in the initial state.

Figures 3 and 4 show the results for a higher intensity ($I=E^2=10^{-2}$ a.u.$=3.54\times10^{14}$ W/cm^{-2}). Figure 3 shows the time evolution of the population of the initial state, 1*s*. Figure 4 indicates the populations of the *s*, *p*, *d*, and *f* states, respectively. Now one clearly sees a spreading of the wave function over different angular-momentum states and a decay of the ground state that does not follow the evolution of the total population of the *s* states. To analyze whether or not this decay indicates ionization, we introduce Fig. 5, which shows the time evolution of the radial distribution of electron population. This kind of figure is not common in the ionization literature, and we consider that it is a simple and precise way to observe how the electron goes away from the nucleus. After a sum over the angular-momentum components, we plot the radius of the spheres that contain given fractions of the electron population inside them. Therefore each curve, labeled by a number between 0.1 and 0.9, indicates the radius of the sphere that contains this fraction of the electron population. For example, the lowest curve of the figure represents the radius of the sphere that contains 10% of the electron population. This radius, r_1, is therefore determined by

$$\sum_{l=0}^{l_{\max}}\int_0^{r_1}|\chi_l(r,t)|^2dr=0.1\ . \tag{14}$$

Analogously, the other radii drawn correspond to fractions $0.2,0.3,\ldots,0.9$ of the total electron population, and we obtain nine curves, $r_1(t),r_2(t),\ldots$ and $r_9(t)$, indicating that, in the space between two consecutive spheres, there is 10% of the electron population.

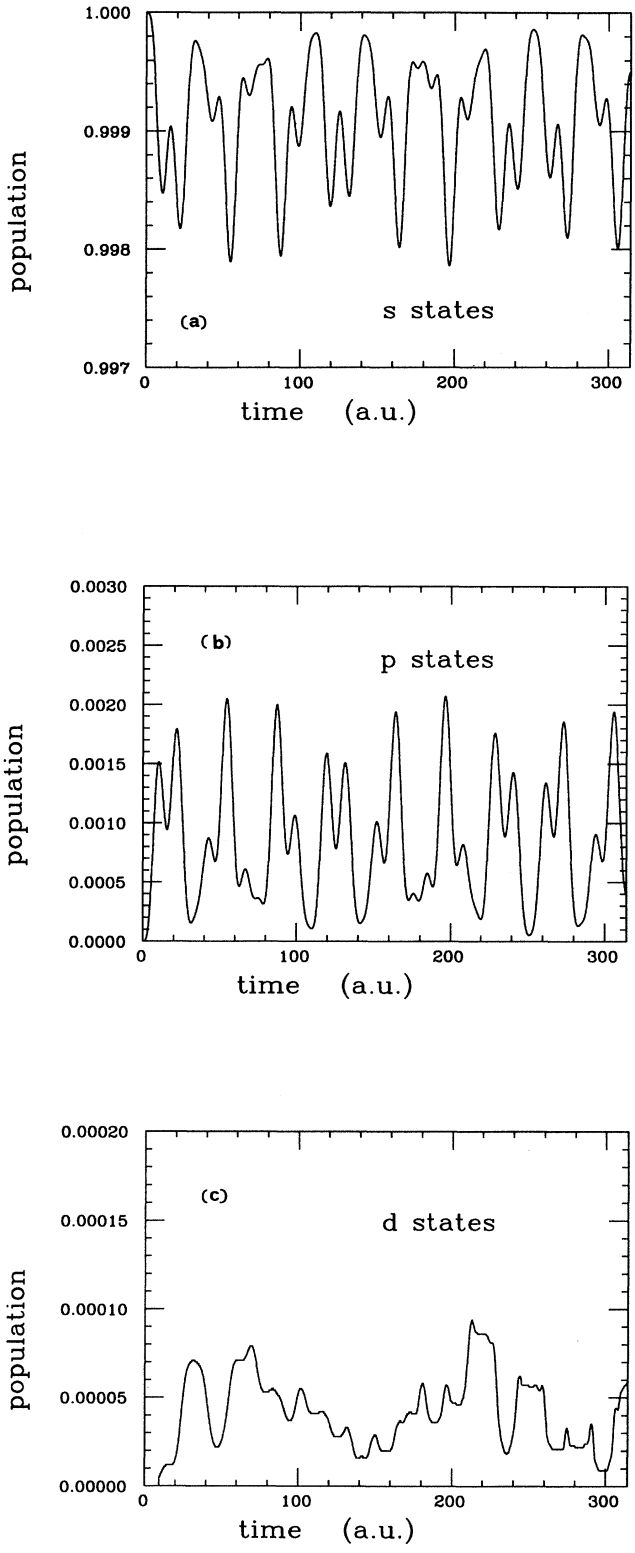

FIG. 2. Time evolution of the populations of the $l=0,1$, and 2 angular-momentum components, i.e., of the populations of the *s*,*p*, and *d* states, respectively, added up for all values of the principal quantum number. All parameters are the same as in Fig. 1.

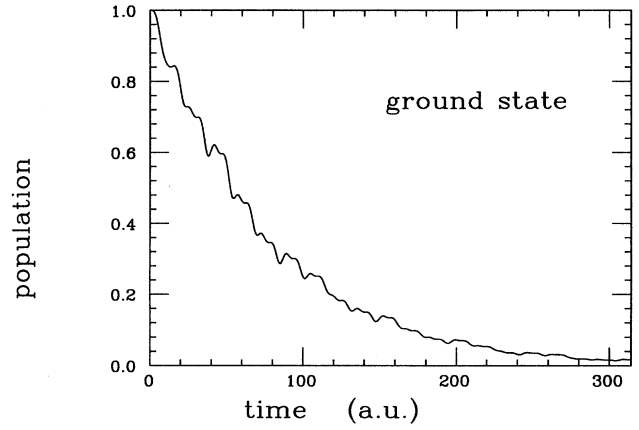

FIG. 3. Time evolution of the ground-state population for a square pulse 100 times more intense than the case of Fig. 1, $E_0=0.1$ a.u.

We consider that this representation of the radial distribution of the population, in this case added up over the angular momentum, is a direct way to identify the main characteristics of the electron dynamics. In particular, this indicates how the electron leaves the central region—close to the nucleus—and shows when the initial-state depletion actually corresponds to fast ionization, as in the case, because the electron population is steadily leaving the vicinity of the nucleus. We have not introduced this kind of figure for the low-intensity case studied at the beginning because, if only one-thousandth of the population is modified from the initial state, the diagram would simply be set of nine horizontal lines.

In our opinion this diagram is very convenient for understanding the dynamics of the ionization process. Of course, a better description is obtained by calculating the ionized population, but this implies a set of projections of the wave function that slow down the speed of computation. Other techniques are used that do not imply projections, like introducing absorbing boundaries and follow-

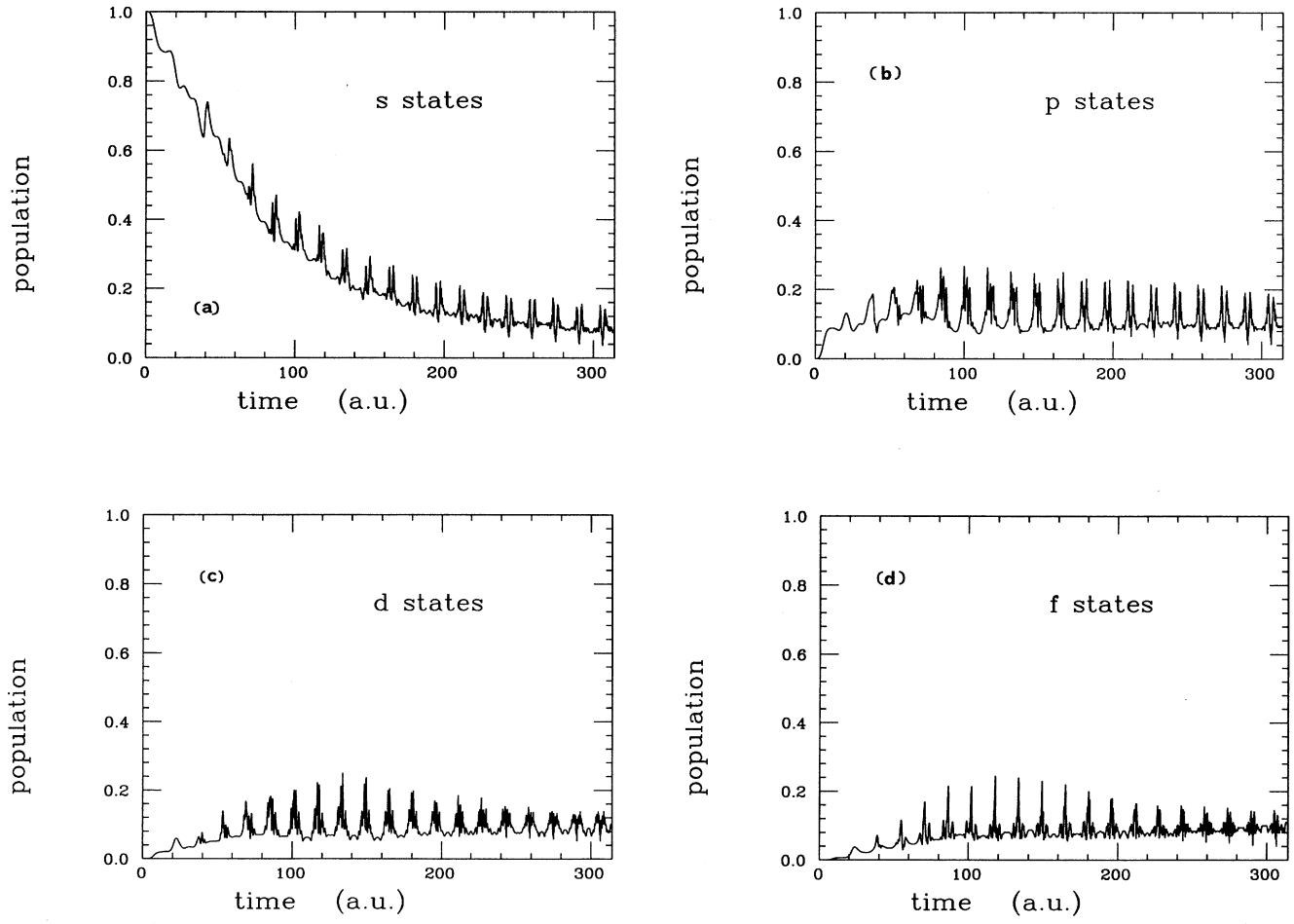

FIG. 4. Time evolution of the populations of the s, p, d, and f states, for the case of Fig. 3, $E_0=0.1$ a.u.

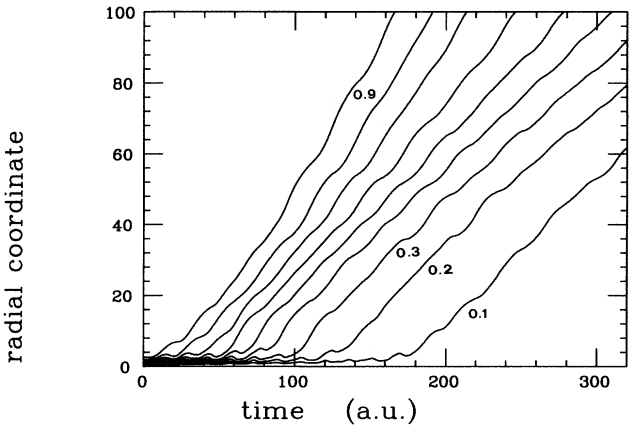

FIG. 5. Radial distribution of the electron population for the case of Figs. 3 and 4, $E_0=0.1$ a.u. Each curve, labeled by a number between 0.1 and 0.9, indicates the radius of the sphere that contains this fraction of the electron populations (added over all the angular-momentum components). Therefore 10% of the electron population is located between each pair of consecutive curves, and we can consider this drawing as a rough representation of the time-dependent distribution of the charge density.

ing the norm of the wave function [13], but these window techniques give less information about the spread of the ionizing electron.

C. Pseudo-one-dimensional results

We have repeated the three-dimensional computations presented in the preceding section, considering now just two angular-momentum components what we have called the pseudo-one-dimensional limit. Figures 6 and 7 show the ground-state population and the total populations of the $l=0$ and 1 states for the same parameters as in Fig. 1 and 2. Because they correspond to $E_0=0.01$ a.u.—that is quite low—and in this case the d states are almost unpopulated, the similitude between both figures can be understood. It is remarkable, however, to have such a good agreement in a system without one-photon resonances from the initial state.

The agreement is not so good for a stronger laser field, as can be seen in Figs. 8 and 9, which are the pseudo-one-dimensional analog of Figs. 3 and 4. For $E_0=0.1$ a.u., in this case, the electron population spreads over different angular-momentum states and, therefore, the truncation of the states with $l=2,3,\ldots$ plays a fundamental role in the dynamics. But many qualitative features of the ionization are still present in the pseudo-one-dimensional limit. This is also clear in Fig. 10, which shows the radial evolution of the electron population, analogously to Fig. 5.

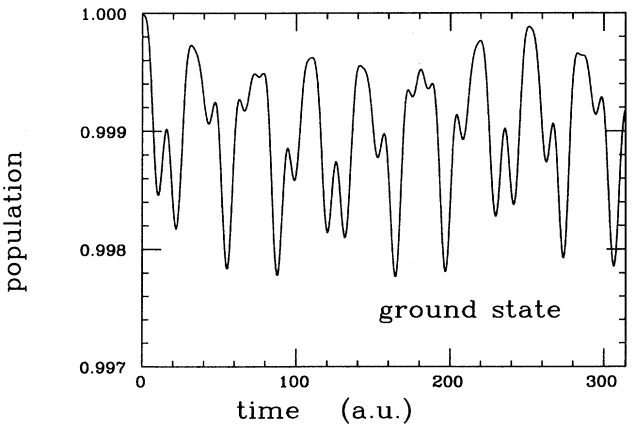

FIG. 6. Time evolution of the ground-state population for the same case as Fig. 1, $E_0=0.01$ a.u., but not computed in the pseudo-one-dimensional limit.

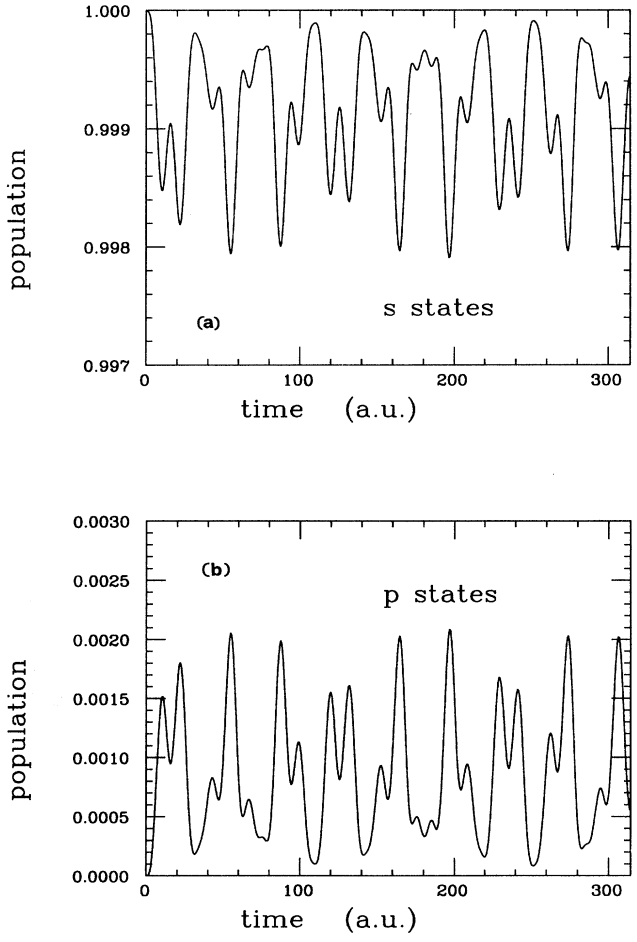

FIG. 7. Time evolution of the populations of the s and p states for the same parameters as in Fig. 2, $E_0=0.01$ a.u., but now computed in the pseudo-one-dimensional limit. The similitude with Fig. 2, the three-dimensional computation, is remarkable. This is so because, for a low-intensity field, angular-momentum components with $l>1$ are almost unpopulated.

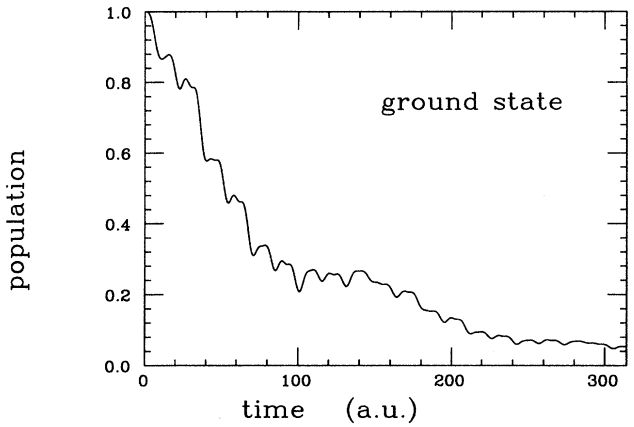

FIG. 8. Time evolution of the ground-state population for the same case as Fig. 3, $E_0=0.1$ a.u., but now computed in the pseudo-one-dimensional limit.

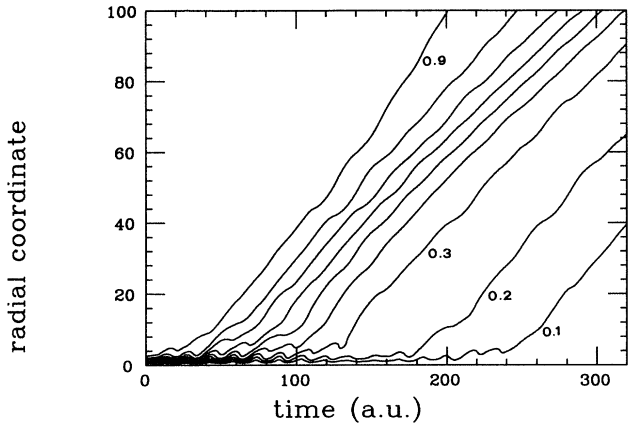

FIG. 10. Radial distribution of the electron population for the case of Figs. 8 and 9, $E_0=0.1$ a.u., in the pseudo-one-dimensional limit. Compare with the three-dimensional result shown in Fig. 5, for the same laser intensity and frequency.

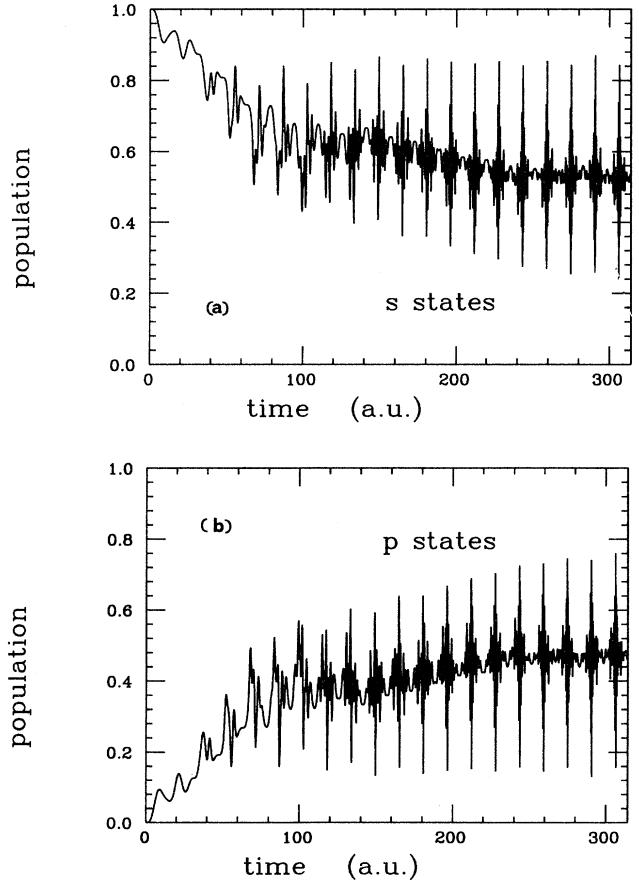

FIG. 9. Time evolution of the populations of the s and p states for the same parameters as in Fig. 4, $E_0=0.1$ a.u., but now computed in the three-dimensional limit. There are certain common features with the three-dimensional case, but the agreement is not as good as it was with a less intense field, because angular-momentum components with $l>1$ carry a significant fraction of the electron population.

D. Harmonic generation

The time-dependent wave function $|\psi(\mathbf{r},t)\rangle$ is used at selected times to compute the expectation value of the dipole moment, $\langle\psi(\mathbf{r},t)|z|\psi(\mathbf{r},t)\rangle=d(t)$; from $d(t)$ we compute the Fourier transform $d(\omega)$ and the spectrum of coherently scattered light is associated with $|d(\omega)|^2$ [14]. The computed spectra are shown in Fig. 11.

The similitude between the pseudo-one-dimensional limit and the three-dimensional result is absolute for low intensities, as happens with the analysis of the electron population. For high laser intensities, both results present some differences, although the main features remain. As the laser intensity increases both results are progressively different due to the population of the states with $l>1$. Nevertheless, the pseudo-one-dimensional model takes into account multiphoton processes of arbitrary order, which allows us to expect high--order harmonic generation not equal but similar to the harmonic generation produced in real hydrogen interacting with linearly polarized light.

It is also clear that the pseudo-one-dimensional model works much better when one considers linearly polarized light. With circularly polarized light an expansion in spherical harmonics is also possible. But in this case two-photon processes would be explicitly excluded in the pseudo-one-dimensional limit.

IV. CONCLUSIONS

We have presented a method to numerically compute ionization of a three-dimensional atom by a linearly polarized laser. The method is based on an expansion of the electron wave function in spherical harmonics. The striking characteristic of this kind of expansion is that, by controlling the number of angular-momentum components in the expansion, it is possible to establish a smooth connection between real three-dimensional atoms and one-dimensional models. From this analysis we for-

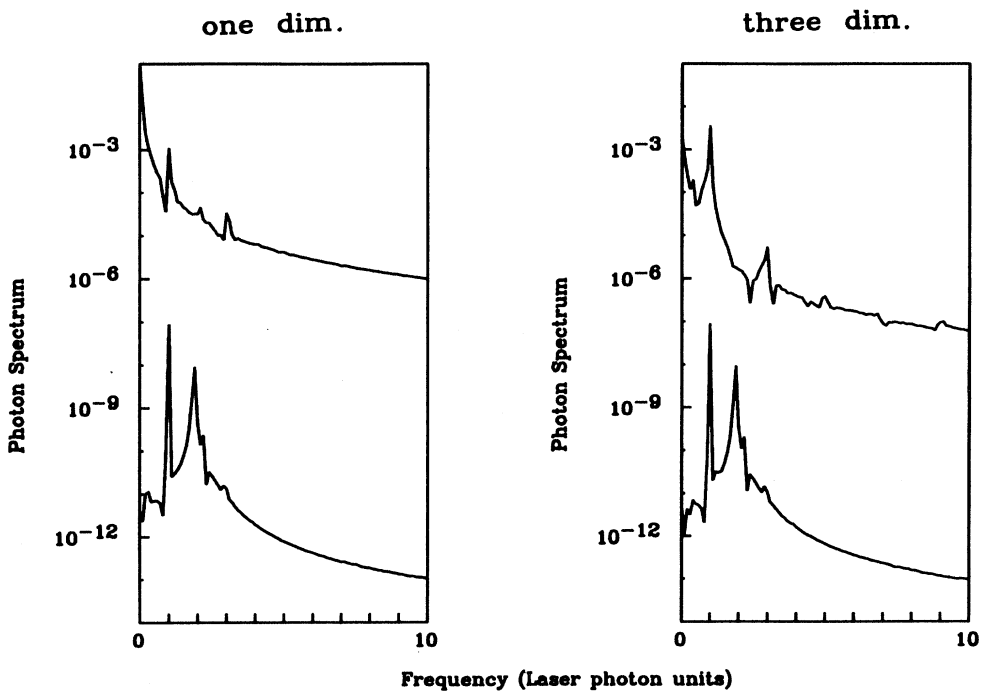

FIG. 11. Harmonic generation calculated for a three-dimensional atom (right) and compared with the pseudo-one-dimensional limit (left), for the two laser intensities studies in this paper. The upper spectra correspond to $E_0=0.1$ a.u. and the lower spectra to $E_0=0.01$ a.u. The photon spectrum is in logarithmic scale, with arbitrary units.

mulate a new limit, the pseudo-one-dimensional limit that, having the same complexity as a one-dimensional model, is closely related to real hydrogen interacting with a linearly polarized laser. We conclude that the pseudo-one-dimensional limit is a good starting point to begin numerical simulations without excessive computing requirements.

ACKNOWLEDGMENTS

We want to thank J. H. Eberly, K. Rzążewski, Q. Su, and A. Bramón for valuable comments and discussions about the subject of this paper. We acknowledge partial support from the Spanish Dirección General de Investigación Científica y Tecnológica (DGICYT Grant No. PB 89 0319 C03 01).

[1] For a recent collection of papers on the subject see, for example, J. Opt. Soc. Am. B **7**, April (1990).
[2] S. Geltman, J. Phys. B **10**, 831 (1977).
[3] J. H. Eberly, Q. Su, and J. Javanainen, J. Opt. Soc. Am. B **6**, 1289 (1989).
[4] J. Javanainen and J. H. Eberly, Phys. Rev. A **39**, 458 (1989).
[5] K. J. LaGattuta, Phys. Rev. A **40**, 683 (1989).
[6] W. G. Greenwood and J. H. Eberly, Phys. Rev. A **43**, 525 (1990).
[7] P. L. DeVries, J. Opt. Soc. Am. B **7**, 517 (1990).
[8] K. J. LaGattuta, J. Opt. Soc. Am. B **7**, 639 (1990).
[9] J. Javanainen, J. H. Eberly, and Q. Su, Phys. Rev. A **38**, 3430 (1988); Q. Su, J. H. Eberly, and J. Javanainen, Phys. Rev. Lett. **64**, 682 (1990); Q. Su and J. H. Eberly, Phys. Rev. A **43**, 2474 (1991).
[10] T. P. Grozdanov, P. S. Krstic, and M. H. Mittleman, Phys. Lett. A **149**, 144 (1990).
[11] A. Sanpera and L. Roso-Franco, Phys. Rev. A **41**, 6515 (1990).
[12] M. S. Pindzola and M. Dörr, Phys. Rev. A **43**, 439 (1991).
[13] K. C. Kulander, K. J. Schafer, and J. L. Krause, in *Multiphoton Processes,* edited by G. Mainfray and P. Agostini (CEA, Saclay, 1990), p. 119.
[14] J. H. Eberly, Q. Su. J. Javanainen, K. C. Kulander, B. W. Shore, and L. Roso-Franco, J. Mod. Opt. **36**, 829 (1989).